

Article

Impact of the Coronavirus Pandemic Lockdown on Atmospheric Nanoparticle Concentrations in Two Sites of Southern Italy

Adelaide Dinoi ^{1,*}, Daniel Gulli ², Ivano Ammoscato ², Claudia R. Calidonna ² and Daniele Contini ¹

¹ Institute of Atmospheric Sciences and Climate, ISAC-CNR, S. P. Lecce-Monteroni km 1.2, 73100 Lecce, Italy; d.contini@isac.cnr.it

² Institute of Atmospheric Sciences and Climate, ISAC-CNR, Zona Industriale, Comparto 15, 88046 Lamezia Terme, Italy; d.gulli@isac.cnr.it (D.G.); i.ammoscato@isac.cnr.it (I.A.); cr.calidonna@isac.cnr.it (C.R.C.)

* Correspondence: a.dinoi@isac.cnr.it

Abstract: During the new coronavirus infection outbreak, the application of strict containment measures entailed a decrease in most human activities, with the consequent reduction of anthropogenic emissions into the atmosphere. In this study, the impact of lockdown on atmospheric particle number concentrations and size distributions is investigated in two different sites of Southern Italy: Lecce and Lamezia Terme, regional stations of the GAW / ACTRIS networks. The effects of restrictions are quantified by comparing submicron particle concentrations, in the size range from 10 nm to 800 nm, measured during the lockdown period and in the same period of previous years, from 2015 to 2019, considering three time intervals: prelockdown, lockdown and postlockdown. Different percentage reductions in total particle number concentrations are observed, -19% and -23% in Lecce and -7% and -4% in Lamezia Terme during lockdown and postlockdown, respectively, with several variations in each subclass of particles. From the comparison, no significant variations of meteorological factors are observed except a reduction of rainfall in 2020, which might explain the higher levels of particle concentrations measured during prelockdown at both stations. In general, the results demonstrate an improvement of air quality, more conspicuous in Lecce than in Lamezia Terme, during the lockdown, with a differed reduction in the concentration of submicronic particles that depends on the different types of sources, their distance from observational sites and local meteorology.



Citation: Dinoi, A.; Gulli, D.; Ammoscato, I.; Calidonna, C.R.; Contini, D. Impact of the Coronavirus Pandemic Lockdown on Atmospheric Nanoparticle Concentrations in Two Sites of Southern Italy. *Atmosphere* **2021**, *12*, 352. <https://doi.org/10.3390/atmos12030352>

Academic Editor: Mikhail Arshinov

Received: 5 February 2021

Accepted: 2 March 2021

Published: 8 March 2021

Publisher's Note: MDPI stays neutral with regard to jurisdictional claims in published maps and institutional affiliations.



Copyright: © 2021 by the authors. Licensee MDPI, Basel, Switzerland. This article is an open access article distributed under the terms and conditions of the Creative Commons Attribution (CC BY) license (<https://creativecommons.org/licenses/by/4.0/>).

Keywords: COVID-19; lockdown; reduced emissions; air quality; nanoparticle concentrations

1. Introduction

The year 2020 will be remembered as the year in which the entire human race was hit by an unknown pandemic: COVID-19. The new coronavirus infection was first identified on 30 December 2019 in China but quickly expanded to other countries, including Europe and the United States, reaching global proportions. Cases rapidly spread in Italy, France and Spain, and on 11 March 2020, the World Health Organization declared it a global pandemic [1]. The governments of many countries, including the Italian government, since the end of February 2020, have adopted increasingly stringent measures in order to try to isolate infected cases, slow down its rate of spread and stop the transmission of the virus [2]. New restrictions such as a reduction in personal travel, social activities (restaurants, theaters, cinemas and sports) and the closure of activities in commercial, industrial and transport (road and air) sectors were imposed. Only some mandatory activities have been partially maintained. Consequently, this has resulted in the decline of most of the polluting sources and a reduction in anthropogenic emissions into the atmosphere. A substantial improvement in air quality was observed in several European countries [3–10], and the skies of many polluted cities around the world quickly have become blue, in

some cases for the first time in people's lives. The reduction of concentrations of the main pollutants, from particulate matter (PM_x) to carbon monoxide (CO), nitrogen dioxide (NO₂) and sulfur dioxide (SO₂), was measured especially in metropolitan areas subject to intense traffic [11]. For instance, Kumari et al. [12] analyzed the effects of lockdown on air quality in 12 major cities around the world, reporting notable reductions in PM_x, NO₂, SO₂ and O₃ concentrations. Similarly, Sharma et al. [13] found an improvement in the air quality of 22 Indian cities due to a reduction in the emission levels of PM_x, CO and NO₂. Pata [14] recorded a decrease of PM_{2.5} emissions in eight different US cities during the pandemic, and Agarwal et al. [15] observed a drastic reduction of atmospheric pollution in six megacities of India and six cities of China. Habibi et al. [7] found high reductions, 63% (Wuhan, China), 61% (Lima, Peru) and 61% (Berlin, Germany), of NO₂, CO and PM_{2.5} levels, respectively.

On the other side, as documented by space observations and ground-based in situ measurements [16–18], the timing and the magnitude of pollutant decreases differed according not only to lockdown measures applied in each country but also to the typology of emission sources, atmospheric chemistry reactions and meteorological conditions [19–22]. By the end of May, lockdown restrictions were relaxed and some economic activities restarted, consequently diminishing the pandemic's effects on atmospheric emissions.

Italy was one of the most severely affected countries in the first phase of the pandemic and one of the first in Europe to have adopted restrictions measures to contain the transmission of the virus. This represented an unprecedented opportunity to investigate the impact of lockdown restrictions on air quality, especially in the most polluted Italian cities [8,23,24].

Despite numerous studies on the impact of lockdown on air quality, to date, few investigations have been performed on the reduction of aerosol particle number concentration [25–27], which, as well known, presents a better indicator of air quality and health effects of particulates compared to mass concentrations [28,29]. For this purpose, in this study, we evaluated the impact of the COVID-19 pandemic outbreak on atmospheric particles, investigating the variation in size distribution and number concentrations of submicron particles before, during and after the lockdown, in two cities of southern Italy. In comparison with analog periods in the previous five years, we quantified the differences and verified if this reduction occurred to a similar degree in both sites. We also explored additional factors such as the effect of local and mesoscale weather patterns (temperature, relative humidity, precipitation and wind speed and direction) that may have influenced the ground-level concentration number and the differences observed between the two periods in the two sites.

2. Methodology: Sites and Instruments

2.1. Study Area

The study was conducted at two observatories, Lecce (ECO, 40.20 N, 18.07 E) and Lamezia Terme (LMT, 38.88 N, 16.23 E), both regional stations of GAW/ACTRIS Networks (Figure 1). Lecce, with 95,000 inhabitants and an area of 238 km², is a town in Puglia's Salento peninsula, and Lamezia Terme (usually called only Lamezia) is a small town of the Calabria region that covers an area of 160 km² and has a population of 70,452 inhabitants.



Figure 1. Position of the two environmental observatories analyzed in this work: Lamezia Terme (LMT) and Lecce (ECO).

The ECO observatory (40.3° N 18.1° E; 36 m a.s.l.) is positioned on the roof of the Institute of Atmospheric Sciences (ISAC-CNR), inside the University Campus [30]. This urban background site is located about 5 km southwest of the municipality of Lecce, roughly 500 m away from important provincial roads, and subject to intense traffic volumes, which combine with the traffic inside the campus. Emissions from vehicular traffic and biomass combustions are among the main local sources of pollution in the site to which are added both natural and anthropogenic long-range contributions [31].

The LMT observatory (38.8° N 16.2° E; 6 m a.s.l.) is a coastal site located about 10 km from the urban city and about 600 m inland the Tyrrhenian coastline. This area, classified as a suburban site, is affected by anthropogenic pollution emissions arising mainly from the agriculture and transport sectors, such as vehicular traffic, the nearby airport and cruises from/to Gioia Tauro. Due to its coastal location and rather flat terrain, air pollutants generated in the city area are often diluted efficiently by wind from the sea. Local meteorology is indeed influenced by a complex system of breezes that develop perpendicularly to the coast, determining a daily variability of atmospheric circulation and the development of vertical structures inside the planetary boundary layer [32], except during perturbations, prevalently from West–Northwest (sea) and less often from East–Northeast (land), where, in both cases, background influence is more relevant [33].

2.2. Measurements Method

Measurements were collected at the ECO and LMT observatories using the same instrument: a TROPOS-type custom-built MPSS [34], designed and manufactured according to EUSAAR/ACTRIS. The two MPSS are equipped with a bipolar diffusion charger, a differential mobility analyzer (Vienna-type DMA, 28 cm length) and a condensation particle counter (CPC, model: TSI 3772, TSI Inc., Rome, Italy). The two instruments measure the number size distribution of particles between 10 and 800 nm by counting particles of the different sizes that are selected based on their electrical mobility and complete a measurement in 5 min. To check the performance of both instruments, daily maintenance, calibration and quality control were done applying the same standard operating procedure [35]. All data were corrected for diffusional particle losses and negatively charged particles according to the recommendations by Wiedensohler et al. [35].

Meteorological parameters, namely temperature (T) relative humidity (RH), rain, wind speed (WS) and direction (WD), were monitored by two identical automatic weather stations, a Vaisala WXT 520 (Vaisala Oyj, Helsinki, Finland) located in each observatory.

3. Results and Discussion

3.1. Variation of Particle Number Concentrations

For each observatory, particle number concentration (PNC) was analyzed considering three different time intervals, each characterized by ~10 weeks: before lockdown (BLD), from 1 January to 9 March 2020; during lockdown (LD), from 10 March to 17 May 2020; and postlockdown (PLD), from 18 May to 31 July 2020. The same time intervals were analyzed for the previous years, from 2015 to 2019, considered as the reference period (REF).

The estimation of total PNC and its subfractions helped us to investigate the roles of various sources. Total particle number size distribution was assumed to have three main modal structures, namely a nucleation mode ($D_p < 20$ nm; D_p = particle diameter), an Aitken mode (20 nm $< D_p < 100$ nm) and an accumulation mode (100 nm $< D_p < 800$ nm). The preliminary data evaluation, comprising arithmetic means ± 1 standard deviation and medians and percentiles (25–75th) of PNC obtained in the two sites, is summarized in Table 1. Differences between 2020 and the reference years were tested by the Mann–Whitney U test. All statistical tests were two sided, and $p < 0.05$ was considered statistically significant.

Table 1. Arithmetic means ± 1 standard deviation and medians (25–75th) percentiles of the total (10 nm $< D_p < 800$ nm), accumulation (100 nm $< D_p < 800$ nm), Aitken (20 nm $< D_p < 100$ nm) and nucleation ($D_p < 20$ nm) number concentrations (cm^{-3}) for the reference (2015–2019) and 2020 years.

ECO	REF			2020		
	BLD	LD	PLD	BLD	LD	PLD
N_{TOT}	$(9.5 \pm 2.3) \times 10^3$ 6840 (3980–12,800)	$(6.9 \pm 1.5) \times 10^3$ 5550 (3580–8740)	$(6.7 \pm 0.9) \times 10^3$ 5560(3830–8200)	$(10.3 \pm 4.1) \times 10^3$ 7580 (4330–1500)	$(5.6 \pm 2.3) \times 10^3$ 4400 (2810–7030)	$(5.1 \pm 2.3) \times 10^3$ 4160(2875–6470)
N_{ACC}	$(2.7 \pm 1.2) \times 10^3$ 1280 (701–3300)	$(1.8 \pm 0.5) \times 10^3$ 1310 (800–2140)	$(1.8 \pm 0.4) \times 10^3$ 1620 (1080–2340)	$(3.2 \pm 2.2) \times 10^3$ 1560 (733–4590)	$(1.8 \pm 1.1) \times 10^3$ 1210 (734–2140)	$(1.2 \pm 0.5) \times 10^3$ 1040 (709–1500)
N_{AIT}	$(5.3 \pm 1.2) \times 10^3$ 3780 (2250–6910)	$(3.8 \pm 0.8) \times 10^3$ 2990 (1940–4750)	$(3.2 \pm 0.4) \times 10^3$ 2730 (1870–4040)	$(5.7 \pm 2.1) \times 10^3$ 4060 (2280–7880)	$(3.1 \pm 1.3) \times 10^3$ 2400 (1560–3820)	$(2.6 \pm 0.9) \times 10^3$ 2220 (1500–3410)
N_{NUC}	$(1.5 \pm 0.4) \times 10^3$ 894 (460–1790)	$(1.4 \pm 0.3) \times 10^3$ 770 (378–1600)	$(1.6 \pm 0.5) \times 10^3$ 762 (387–1590)	$(1.5 \pm 0.7) \times 10^3$ 799 (425–1640)	$(0.6 \pm 0.5) \times 10^3$ 290 (139–682)	$(1.3 \pm 0.9) \times 10^3$ 530 (254–1200)
LMT	REF			2020		
	BLD	LD	PLD	BLD	LD	PLD
N_{TOT}	$(5.6 \pm 1.6) \times 10^3$ 3567(1818–7284)	$(5.5 \pm 1.9) \times 10^3$ 3663 (2510–6089)	$(4.5 \pm 1.2) \times 10^3$ 3154 (2296–5200)	$(6.7 \pm 3.4) \times 10^3$ 4303 (2325–9043)	$(5.1 \pm 1.8) \times 10^3$ 4028 (2592–6238)	$(4.4 \pm 1.5) \times 10^3$ 3146 (2208–5032)
N_{ACC}	$(1.2 \pm 0.5) \times 10^3$ 690 (338–1436)	$(1.3 \pm 0.5) \times 10^3$ 1067 (600–1533)	$(1.1 \pm 0.2) \times 10^3$ 1142 (799–1439)	$(1.5 \pm 0.8) \times 10^3$ 1010 (535–1844)	$(1.2 \pm 0.6) \times 10^3$ 1044 (650–1633)	$(0.7 \pm 0.2) \times 10^3$ 660 (502–921)
N_{AIT}	$(2.8 \pm 0.8) \times 10^3$ 1812 (903–3471)	$(2.7 \pm 1.0) \times 10^3$ 1914 (1293–3089)	$(2.0 \pm 0.6) \times 10^3$ 1502 (1061–2393)	$(3.1 \pm 1.5) \times 10^3$ 2020 (1152–4082)	$(2.5 \pm 0.8) \times 10^3$ 2073 (1390–2923)	$(2.1 \pm 0.9) \times 10^3$ 1680 (1190–2352)
N_{NUC}	$(1.7 \pm 0.6) \times 10^3$ 765 (302–1966)	$(1.5 \pm 0.9) \times 10^3$ 613 (193–1573)	$(1.3 \pm 0.7) \times 10^3$ 474 (100–1465)	$(2.1 \pm 1.6) \times 10^3$ 978(369–2514)	$(1.4 \pm 0.9) \times 10^3$ 644 (246–1573)	$(1.6 \pm 0.9) \times 10^3$ 682 (228–1856)

Temporal variability of daily number concentrations during the study period is shown in Figure 2, where data collected during the year 2020 (orange lines) and daily average values collected during the reference period, gray and blue lines for the ECO and LMT sites, respectively, are compared.

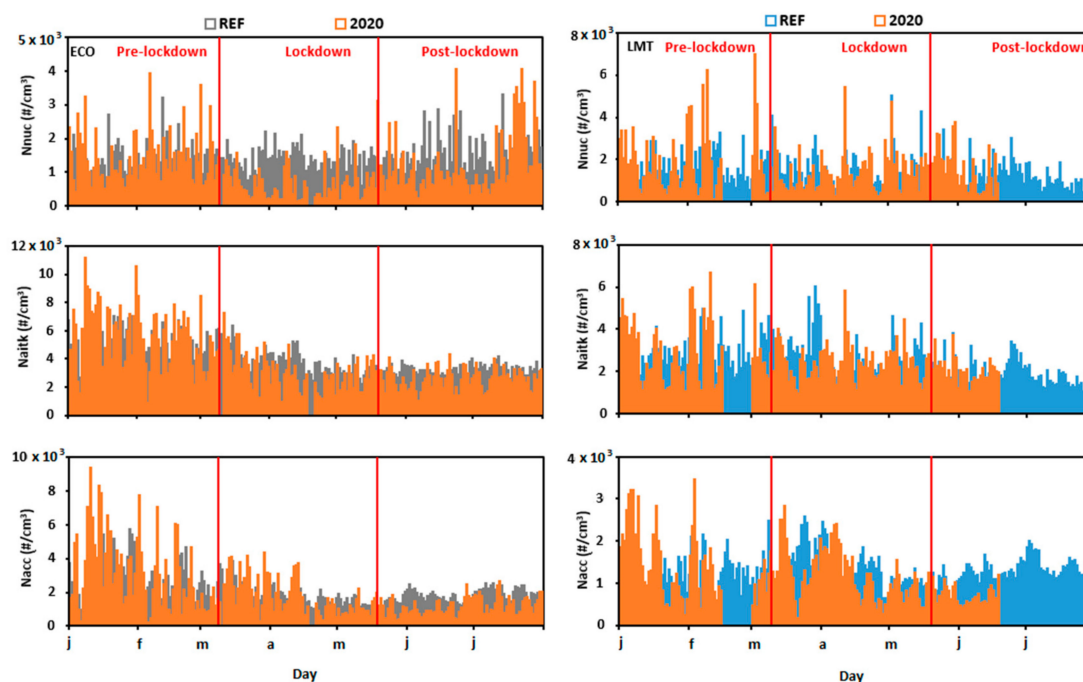


Figure 2. Comparison of daily variation of particle number concentration (PNC) for each size range (N_{nuc} ($D_p < 20$ nm), N_{aitk} (20 nm $< D_p < 100$ nm) and N_{acc} (100 nm $< D_p < 800$ nm)) at ECO (on the left) and LMT (on the right). The red lines refer to 2020, and the grey and blue lines refer to reference years (2015–2019), respectively.

Due to technical/maintenance problems, at the end of April and June 2020, some measurements at the LMT site were not carried out, as shown in Figure 2 (missing data). At a glance, we can observe a similar trend in both sites; in fact, the contribution of each size mode to the total particle remains almost unchanged between 2020 and the reference years. The average contributions of nucleation, Aitken and accumulation particles to total PNC in ECO were, respectively, 12–25%, 48–56% and 26–32%, and in LMT, they were 27–35%, 44–50% and 16–24%. In both sites, total number concentrations were dominated by the Aitken particle fraction, which is in agreement with several studies [36–38]. The largest contribution of Aitken mode particles highlights that both sites are affected by aerosol emitted by traffic and the burning of biomass, especially in cold months, where this last emission source is more relevant according to previous source apportionment analysis [31]. After Aitken particles, the highest percentage of accumulation mode particles, resulting from aged aerosol, road dust resuspension and brake wear, may be due to the proximity of ECO site to the roads, while the highest percentage of nucleation mode particles in LMT indicates that the site is mainly affected by fresh particles. We think that the effects of the different distances of the sites from the main anthropogenic sources as well as local meteorology play a decisive role in the type of observed particles and their concentrations.

The variability of ambient submicronic particle size and concentrations depends on the dispersion conditions governed by wind speed and direction, temperature and the local orography, which favor the exchange of polluted air within the lowest part of the urban boundary layer [39,40]. Looking at the data, it can be seen that the total particles at the ECO ($7.7 \times 10^3 \text{ cm}^{-3}$) averaged about 1.5 times the level recorded at LMT ($5.2 \times 10^3 \text{ cm}^{-3}$) during the reference years.

In order to assess the emission changes due to the reduction of anthropogenic activities, the relative percentage differences between 2020 and the reference years were derived by means of the PNC variation calculated as follows:

$$\text{PNC}_{\text{variation}} = [(\text{PNC}_{20} - \text{PNC}_{\text{ref}}) / \text{PNC}_{\text{ref}}] \times 100$$

where PNC_{20} and PNC_{ref} represent the particle number concentration related to 2020 and the reference years, respectively. The percentage change was calculated for each mode and is shown in Figure 3. During the lockdown period, the ratio was -53% , -17% and $+4\%$ in ECO and -6% , -9% and -2% in LMT, for N_{nuc} , N_{aitk} and N_{acc} , respectively. The ECO site exhibited a more marked reduction (statistically significant for N_{nuc} $p < 0.0001$ and N_{aitk} $p < 0.0003$) than LMT (not statistically significant), probably because the area is particularly affected by emissions from road vehicles [30], whose use was very limited during the lockdown. According to road mobility data, an average reduction in vehicles of -55% in Lecce and -50% in Lamezia was observed during the lockdown period. Daily reductions, by country, retrieved by the online platform developed for Italy by EnelX and Here [41], are normalized against a baseline taken as a median and corresponding to the five-week period before the lockdown.

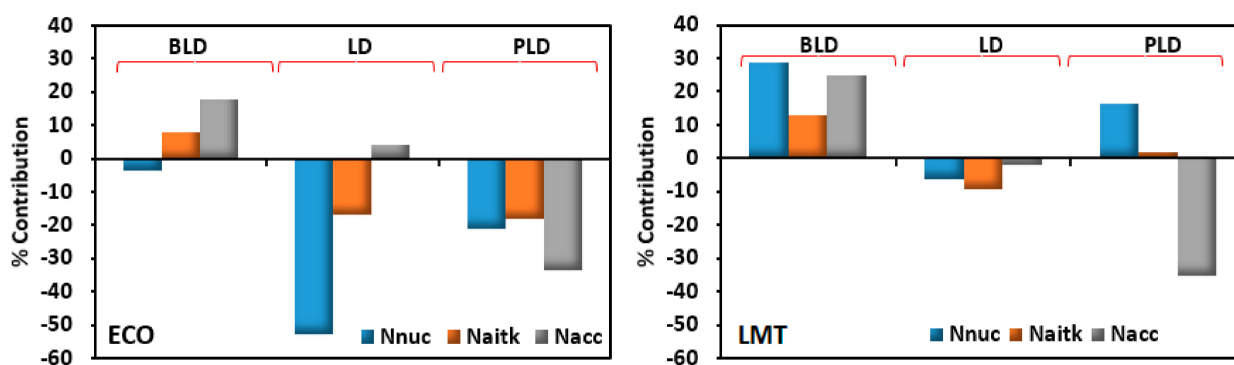


Figure 3. Percentage variation ratio for both sites, ECO and LMT, during the three time windows for each size class: N_{nuc} ($D_p < 20$ nm), N_{aitk} (20 nm $< D_p < 100$ nm) and N_{acc} (100 nm $< D_p < 800$ nm).

The effect of reduction in traffic emissions was still evident during the PLD period, mostly in ECO (statistically significant for each fraction), as shown by the unaffected percentage (-18%) of N_{aitk} and the increased percentage (-33%) of N_{acc} , arising also from fine mineral/soil dust linked to road traffic [42]. Online data shows that the postlockdown period starts with a reduction in vehicles of -12% in Lecce and -28% in Lamezia.

It is important to point out that emissions are the result of different factors including the number and type of vehicles, the type of fuel used, the travel behavior and the distance traveled by each vehicle [43]. Though inside the campus the situation remained unchanged, with educational and research activities suspended and the consequent containment of circulating vehicles, during the PLD, the moderate recovery of activities was followed by a resumption of travel and of circulating vehicles (especially of a certain type) in the nearby roads, which could explain these results. The different percentage variation of N_{nuc} (-21%) observed during PLD could instead be related to new particulate formation events, more frequent during warm months, as already observed in Dinoi et al. [30,44].

It is interesting to note that despite the lockdown, LMT recorded minor percentage reductions. Primarily because the site is not mainly affected by direct anthropogenic emissions, as prevalent circulation is opposite to possible emission sources. The observatory is about 10 km away from the inner city of Lamezia and, except the two main emission sources, the International Airport of Lamezia and the highway, located about 4–5 km from the observatory, respectively, no other important sources of air pollution are present in the vicinity. Furthermore, it is a marine-coastal site and can benefit from the effects of sea breezes [33]. Continuous mixing with cleaner (marine) air masses guarantees a good dispersion of pollutants and a reduction in concentrations. During the PLD was observed a slight increase, $+16\%$, -1.7% -35% for N_{nuc} , N_{aitk} and N_{acc} respectively (significant only for N_{nuc} and N_{acc}). Except N_{aitk} that exhibited a different behavior, N_{nuc} and N_{acc} showed the same trend observed in ECO with an increase of percentage twice with respect to LD. The different percentage ratios show the effect of the reduction of anthropogenic activities,

in particular traffic emissions, during the lockdown and the slow recovery during the PLD. These trends were also confirmed by particle size distribution (Figure 4) where each site exhibited similar curves between reference and 2020 years (even if more smoothed in reference years perhaps due to the averaging effect), except PLD curves that showed greater variability in both sites.

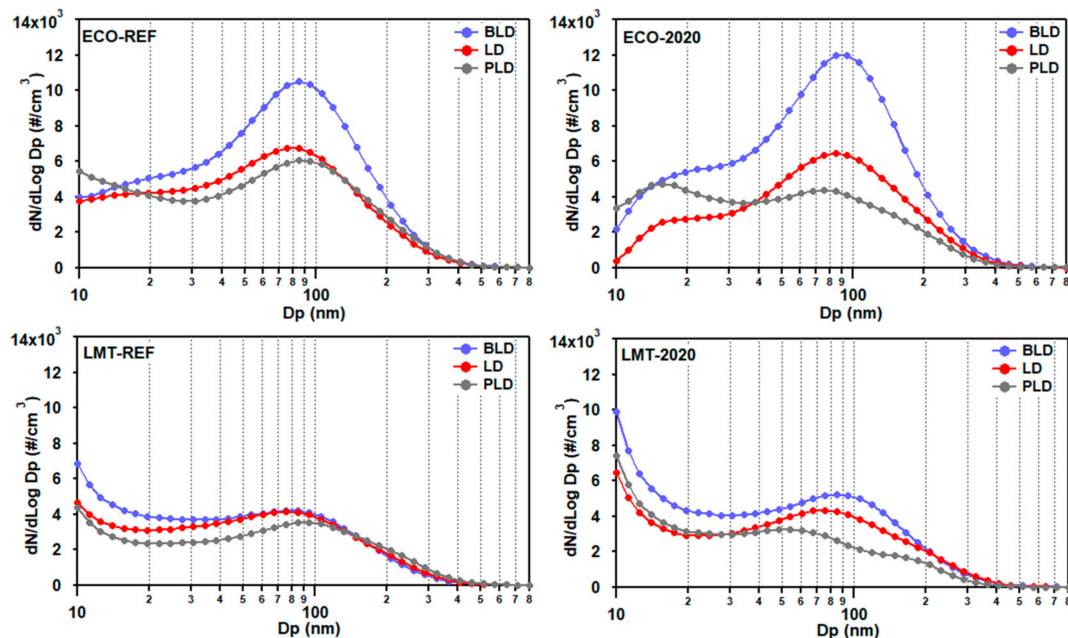


Figure 4. Particle number size distributions average during the three time windows over the reference (2015–2019) and 2020 years for both sites, ECO and LMT.

During the BLD and LD periods, size distributions display a maximum centered on median diameters around 80–90 nm, both in ECO and LMT, in the reference and 2020 years. Instead, during the PLD in the reference years, both sites have a maximum at around 80–90 nm, which has moved toward lower diameters, around 60–70 nm during 2020. Lecce shows a further peak around 15 nm. The variations of particle number size distributions underline not only the different emissions that characterized the pandemic period but also the deep differences between the two observational sites: urban background (ECO) and coastal site (LMT).

3.2. Weekly Trend of Aerosol Concentrations during Lockdown

Weekly trends of number concentrations during the lockdown period were also investigated (Figure 5). The diurnal pattern shows a reduction of particle concentrations throughout the days, but the variability remains almost unchanged, continuing to have morning and evening peaks as in the previous years. Similar behaviors were observed in several cities of the world [45–47]. By comparison, the number concentrations showed a pronounced diurnal cycle, which seems to be time correlated with traffic intensity in both sites and characterized by different levels in each subclass of particles both in 2020 and in the reference period.



Figure 5. Percentage weekly average cycle of particle number concentration, N_{nuc} ($D_p < 20$ nm), N_{aitk} (20 nm $< D_p < 100$ nm) and N_{acc} (100 nm $< D_p < 800$ nm), collected from 10 March to 17 May of 2020 and the reference (2015–2019) years, in ECO and LMT.

Especially at the ECO site, the daily maxima of N_{nuc} and N_{aitk} , around 6:00 a.m., were coincident with the morning traffic rush hour and showed a marked reduction of $\sim 50\%$ in 2020, attributable to the significant reduction in vehicular traffic (-55%). A reduction was also observed in LMT but more limited.

The second important peak of N_{nuc} and N_{aitk} around 8:00 p.m., however, shows no noteworthy decrease at either site. This peak is attributed to the joint contribution of emissions related to domestic heating and late evening traffic rush hours, as confirmed by the collapse of the peak on Sunday observed in ECO, usually connected to the “movida” traffic. The reduction in traffic emissions, during the evening hours, may have been replaced by an increase in domestic heating emissions, since citizens were forced to stay home as long as possible [6].

Another important reduction of $\sim 50\%$ was observed in the midday peak of N_{nuc} , in ECO. As already noted in Dinoi et al. [30,44], this peak between 11:00 and 12:00 a.m., relevant only in spring and summer, is probably due to photochemical processes occurring when climatic conditions and high concentrations of precursor species create suitable conditions to trigger the nucleation and growth process of new aerosol particles. The simultaneous reduction in the concentration of other pollutant compounds (e.g., SO_2 , and VOC), which act as precursors to the formation of secondary aerosol, could then explain the reduction observed in this period.

Regarding N_{acc} , while in LMT, any relevant variation between the two periods was not observed, in ECO, an increase was observed. Accumulation particles show a concentration modulated by the daily trend of the mixing layer height, with a bimodal distribution coincident with the morning and late evening peaks. The higher levels measured in 2020, on the other hand, suggest that the accumulation particles could be associated not only with road traffic (directly through exhaust and nonexhaust emissions and indirectly through the resuspension of dust road) but also with other types of sources and/or processes (secondary aerosol formation and long-range transport). As observed in recent works [48,49], large decreases in NO_x emissions from transportation increased ozone levels and the nocturnal formation of NO_3 radicals. This increased the atmospheric oxidizing capacity facilitating the formation of secondary particulate matter.

Regarding LMT, the smaller variation of the concentrations observed is very interesting if we consider that in this area there has been a reduction not only in the volume of road traffic but also in air traffic (having drastically reduced flights).

We believe that the findings could be due to the fact that the contribution of the two sources has little influence on the measurement site or that the site was affected by other emission sources in that period. People spent more time indoors during the lockdown period making greater use of home heating, for example, which may have compensated or even overwhelmed the lack of emissions from other sources [49].

3.3. Impact of Meteorological Conditions on Particle Concentrations

Meteorological conditions can have a significant effect on the concentration of local air pollution, not only primary particles but also on the formation of secondary aerosols. It was therefore essential to consider the changes in meteorological parameters from year to year and the influence they may have had on the variation of the particle concentrations.

As shown in Figure 6, meteorological data were analyzed for the comparison of the different scenarios. In ECO, average temperatures were measured between 10 and 25 °C, relative humidity between 58% and 72% and wind speed around 2.1 m/s. In LMT, average temperatures were between 12 and 23 °C, relative humidity between 66% and 69% and wind speed between 3.2 and 4.0 m/s. As we can see, negligible differences (no statistically significant) in meteorological factors were found between the three periods of 2020 and of previous years pointing out that they were characterized by comparable meteorological conditions.

However, a marked difference ($p < 0.0001$) has instead been found in rainfall of the BLD period, in both sites. It seems that the first months of 2020 were less rainy than the reference years, with 65% and 100% less rain in ECO and LMT, respectively, and 70% less rain during LD only in LMT.

Rainfall can wash air pollutants out of the atmosphere, especially water-soluble pollutants, such as NO_2 and SO_2 and particulate matter. Therefore, the increase in PNC observed during the BLD period of 2020, especially in LMT, could be partially caused by this lower rainfall during these months. No further investigations have been carried out to explain the higher percentage of particle number concentration observed during the BLD period in LMT because this is not the purpose of this work. The study of weather conditions was completed accounting for wind directions (Figure 7).

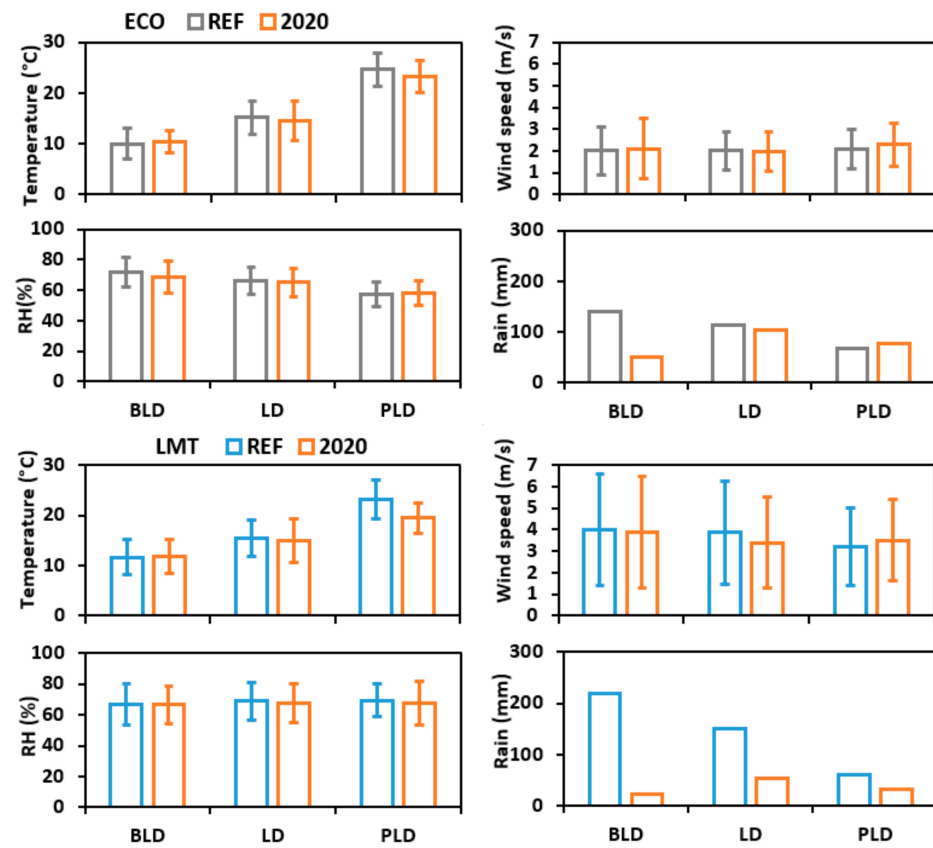


Figure 6. Average values of temperature, relative humidity, wind speed and rain accumulation, measured during the three periods (before lockdown (BLD), lockdown (LD) and postlockdown (PLD)) of 2020 and reference (2015–2019) years.

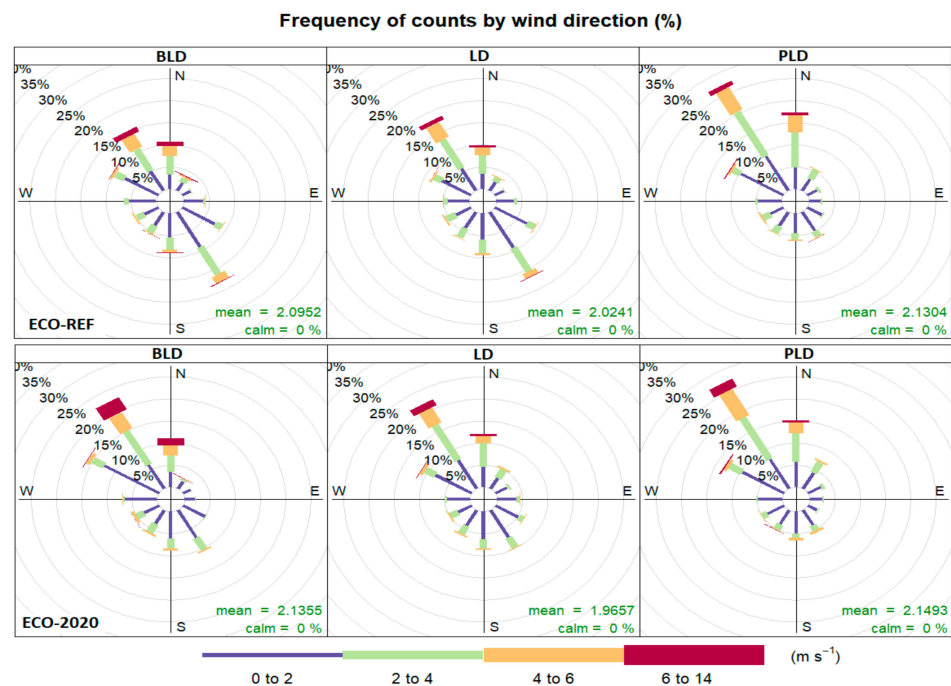


Figure 7. Wind roses related to the three periods (BLD, LD and PLD) of the reference (2015–2019) years and 2020 at the ECO and LMT observatories (from top to down).

The wind rises at the two measurement sites showed similar results between reference years and 2020. In the ECO the dominating wind direction was mainly from N–NNW, with a frequency of occurrence of 15% and 25%, respectively, during 2020, very similar to what observed in reference years, whereas in BLD and LD periods, there is also a component of the wind blowing from the SSE–SE direction.

In LMT, observational data revealed predominant a W and NE wind direction, with a frequency of occurrence of 25–35% and 25%, respectively, both characterized by height wind speed (>6 m/s). The absence of significant differences in meteorological conditions therefore cannot explain the variations in number concentration observed between 2020 and the reference years.

4. Conclusions

In this study, changes in the number concentrations of submicron particles in two towns of southern Italy were investigated, by comparing the data collected before, during and after the 2020 lockdown phase with the average values collected during the years 2015–2019 of the same period.

Although PNC showed similar patterns to the prepandemic period, the total particle number concentrations decreased by –19% and –23% at the ECO site, and –7% and –4% at the LMT site during and after the restriction phases, respectively. Different percentage ratios were also observed in each dimensional subclass of particles with variations from –53% to –21%, about –17% and from +4% to –33% in ECO and from –6% to +16%, from –9% to –2% and from –2% to –35% in LMT, for N_{nuc} , N_{aitk} and N_{acc} , respectively, during and after the lockdown period. These variations cannot be related, or at least not directly, to meteorological factors since the compared periods were characterized by similar meteorological conditions.

This work highlights that, despite the reduction in traffic, industrial emissions and other anthropogenic activities, one site has shown a substantial improvement in air quality while the other has experienced negligible or marginal improvement. The different reduction of the particle number concentrations, observed in the two sites, is mainly traced back to various factors, such as the dominant emission sources, the distance from the observational site and their influence, geographic position and specific meteorological conditions. Therefore, the findings show that the environmental response to the restrictions of most human activities can vary widely according to the characteristics of the observational area.

This suggests that policies aimed at reducing only specific emission sources, such as traffic and industries, could not be equally valid for each area and that ad hoc actions are needed to achieve substantial air quality improvements on a large scale.

Author Contributions: Conceptualization, A.D., D.G., I.A., C.R.C. and D.C.; investigation, A.D. and D.G.; writing—original draft, A.D.; writing—review and editing, A.D., D.G., I.A., C.R.C. and D.C. All authors have read and agreed to the published version of the manuscript.

Funding: This work was supported by the financial contribution of the project I-AMICA (Infrastructure of High Technology for Environmental and Climate Monitoring-PONa3_00363), a project of structural improvement financed under the National Operational Program (NOP) for “Research and Competitiveness 2007–2013” cofunded with the European Regional Development Fund (ERDF) and national resources.

Institutional Review Board Statement: Not applicable.

Informed Consent Statement: Not applicable.

Data Availability Statement: Data sharing not applicable.

Conflicts of Interest: The authors declare no conflict of interest.

References

1. World Health Organization. WHO Director-General's Opening Remarks at the Media Briefing on COVID-19. 2020. Available online: <https://www.who.int/dg/speeches/detail/who-director-general-s-opening-remarks-at-the-media-briefing-on-covid-19> (accessed on 11 March 2020).
2. Guevara, M.; Jorba, O.; Soret, A.; Petetin, H.; Bowdalo, D.; Serradell, K.; Tena, C.; Denier van der Gon, H.; Kuenen, J.; Peuch, V.H.; et al. Time-resolved emission reductions for atmospheric chemistry modelling in Europe during the COVID-19 lockdowns. *Atmos. Chem. Phys.* **2021**, *21*, 773–797. [[CrossRef](#)]
3. Giani, P.; Castruccio, S.; Anav, A.; Howard, D.; Hu, W.; Crippa, P. Short-term and long-term health impacts of air pollution reductions from COVID-19 lockdowns in China and Europe: A modelling study. *Lancet Planet. Health* **2020**, *4*, 474–482. [[CrossRef](#)]
4. European Environmental Agency. Air Pollution Goes Down as Europe Takes Hard Measures to Combat Coronavirus. 2020. Available online: <https://www.eea.europa.eu/highlights/air-pollution-goes-down-as> (accessed on 25 March 2020).
5. Baldasano, J. COVID-19 lockdown effects on air quality by NO₂ in the cities of Barcelona and Madrid (Spain). *Sci. Total Environ.* **2020**, *741*, 140353. [[CrossRef](#)]
6. Menut, L.; Bessagnet, B.; Siour, G.; Mailler, S.; Pennel, R.; Cholakian, A. Impact of lockdown measures to combat Covid-19 on air quality over western Europe. *Sci. Total Environ.* **2020**, *741*, 140426. [[CrossRef](#)]
7. Habibi, H.; Awal, R.; Fares, A.; Ghahremannejad, M. COVID-19 and the Improvement of the Global Air Quality: The Bright Side of a Pandemic. *Atmosphere* **2020**, *11*, 1279. [[CrossRef](#)]
8. Collivignarelli, M.C.; Abba, A.; Bertanza, G.; Pedrazzani, R.; Ricciardi, P.; Miino, M.C. Lockdown for CoViD-2019 in Milan: What are the effects on air quality? *Sci. Total Environ.* **2020**, 139280. [[CrossRef](#)] [[PubMed](#)]
9. Sicard, P.; De Marco, A.; Agathokleous, E.; Feng, Z.; Xu, X.; Paoletti, E.; Diéguez Rodríguez, J.J.; Calatayud, V. Amplified ozone pollution in cities during the COVID-19 lockdown. *Sci. Total Environ.* **2020**, *735*, 139542. [[CrossRef](#)] [[PubMed](#)]
10. Berman, J.D.; Ebisu, K. Changes in US air pollution during the COVID-19 pandemic. *Sci. Total Environ.* **2020**, *739*, 139864. [[CrossRef](#)] [[PubMed](#)]
11. Donzelli, G.; Cioni, L.; Cancellieri, M.; Morales, A.L.; Suárez-Varela, M.M. The Effect of the Covid-19 Lockdown on Air Quality in Three Italian Medium-Sized Cities. *Atmosphere* **2020**, *11*, 1118. [[CrossRef](#)]
12. Kumari, P.; Toshniwal, D. Impact of lockdown on air quality over major cities across the globe during COVID-19 pandemic. *Urban Clim.* **2020**, *34*, 100719. [[CrossRef](#)]
13. Sharma, S.; Zhang, M.; Gao, J.; Zhang, H.; Kota, S.H. Effect of restricted emissions during COVID-19 on air quality in India. *Sci. Total Environ.* **2020**, *728*, 138878. [[CrossRef](#)]
14. Pata, U.K. How is covid-19 affecting environmental pollution in us cities? Evidence from asymmetric fourier causality test. *Air Qual. Atmos. Health* **2020**, *1*, 7.
15. Agarwal, A.; Kaushik, A.; Kumar, S.; Mishra, R.K. Comparative study on air quality status in indian and chinese cities before and during the covid-19 lockdown period. *Air Qual. Atmos. Health* **2020**, *1*, 12. [[CrossRef](#)]
16. Zhang, Z.; Arshad, A.; Zhang, C.; Hussain, S.; Li, W. Unprecedented Temporary Reduction in Global Air Pollution Associated with COVID-19 Forced Confinement: A Continental and City Scale Analysis. *Remote Sens.* **2020**, *12*, 2420. [[CrossRef](#)]
17. European Space Agency (ESA). 2020. Available online: https://www.esa.int/Applications/Observing_the_Earth/Copernicus/Sentinel-5P (accessed on 27 March 2020).
18. Muhammad, S.; Long, X.; Salman, M. COVID-19 pandemic and environmental pollution: A blessing in disguise? *Sci. Total Environ.* **2020**, *728*, 138820. [[CrossRef](#)] [[PubMed](#)]
19. Schiermeier, Q. Why pollution is plummeting in some cities—But not others. *Nature* **2020**, *580*, 313. [[CrossRef](#)] [[PubMed](#)]
20. Brimblecombe, P.; Lai, Y. Subtle Changes or Dramatic Perceptions of Air Pollution in Sydney during COVID-19. *Environments* **2021**, *8*, 2. [[CrossRef](#)]
21. Silver, B.; He, X.; Arnold, S.R.; Spracklen, D.V. The impact of COVID-19 control measures on air quality in China. *Environ. Res. Lett.* **2020**, *15*, 084021. [[CrossRef](#)]
22. Rodríguez-Urrego, D.; Rodríguez-Urrego, L. Air quality during the COVID-19: PM_{2.5} analysis in the 50 most polluted capital cities in the world. *Environ. Pollut.* **2020**, *266*, 115042. [[CrossRef](#)]
23. Putaud, J.P.; Pozzoli, L.; Pisoni, E.; Dos Santos, S.M.; Lagler, F.; Lanzani, G.; Dal Santo, U.; Colette, A. Impacts of the COVID-19 lockdown on air pollution at regional and urban background sites in northern Italy. *Atmos. Chem. Phys.* **2020**. [[CrossRef](#)]
24. Gualtieri, G.; Brilli, L.; Carotenuto, F.; Vagnoli, C.; Zaldei, A.; Gioli, B. Quantifying road traffic impact on air quality in urban areas: A Covid19-induced lockdown analysis in Italy. *Environ. Pollut.* **2020**, *267*, 115682. [[CrossRef](#)] [[PubMed](#)]
25. Shen, X.; Sun, J.; Yu, F.; Zhang, X.; Zhang, Y.; Hu, X.; Xia, C.; Zhang, S. Enhancement of nanoparticle formation and growth during the COVID-19 lockdown period in urban Beijing. *Atmos. Chem. Phys.* **2020**. Preprint. [[CrossRef](#)]
26. Hudda, N.; Matthew, C.; Patton, S.A.P.; Durant, J.L. Reductions in traffic-related black carbon and ultrafine particle number concentrations in an urban neighborhood during the COVID-19 pandemic. *Sci. Total Environ.* **2020**, *742*, 140931. [[CrossRef](#)]
27. Dai, Q.; Ding, J.; Song, C.; Liu, B.; Bi, X.; Wu, J.; Zhang, Y.; Feng, Y.; Hopke, P.K. Changes in source contributions to particle number concentrations after the COVID-19 outbreak: Insights from a dispersion normalized PMF. *Sci. Total Environ.* **2021**, *759*, 143548. [[CrossRef](#)]
28. Englert, N. Fine particles and human health a review of epidemiological studies. *Toxicol. Lett.* **2004**, *149*, 235–242. [[CrossRef](#)]

29. Vu, T.; Zauli-Sajani, S.; Poluzzi, V.; Harrison, R.M. Factors controlling the lung dose of road traffic-generated sub-micrometre aerosols from outdoor to indoor environments. *Air Q. Atmos. Health* **2018**, *11*, 615–625. [[CrossRef](#)]
30. Dinoi, A.; Conte, M.; Grasso, F.M.; Contini, D. Long-Term Characterization of Submicron Atmospheric Particles in an Urban Background Site in Southern Italy. *Atmosphere* **2020**, *11*, 334. [[CrossRef](#)]
31. Cesari, D.; De Benedetto, G.E.; Bonasoni, P.; Busetto, M.; Dinoi, A.; Merico, E.; Chirizzi, D.; Cristofanelli, P.; Donato, A.; Grasso, F.M.; et al. Seasonal variability of PM_{2.5} and PM₁₀ composition and sources in an urban background site in Southern Italy. *Sci. Total Environ.* **2018**, *612*, 202–213. [[CrossRef](#)]
32. Cristofanelli, P.; Busetto, M.; Calzolari, F.; Ammoscato, I.; Gulli, D.; Dinoi, A.; Calidonna, C.R.; Contini, D.; Sferlazzo, D.; Di Iorio, T.; et al. Investigation of reactive gases and methane variability in the coastal boundary layer of the central Mediterranean basin. *Elem. Sci. Anthr.* **2017**, *5*, 12. [[CrossRef](#)]
33. Calidonna, C.R.; Avolio, E.; Gulli, D.; Ammoscato, I.; De Pino, M.; Donato, A.; Lo Feudo, T. Five Years of Dust Episodes at the Southern Italy GAWRegional Coastal Mediterranean Observatory: Multisensor and Modelling Analysis. *Atmosphere* **2020**, *11*, 456. [[CrossRef](#)]
34. Wiedensohler, A.; Birmili, W.; Nowak, A.; Sonntag, A.; Weinhold, K.; Merkel, M.; Wehner, B.; Tuch, T.; Pfeifer, S.; Fiebig, M.; et al. Mobility particle size spectrometers: Harmonization of technical standards and data structure to facilitate high quality long-term observations of atmospheric particle number size distributions. *Atmos. Meas. Tech.* **2012**, *5*, 657–685. [[CrossRef](#)]
35. Wiedensohler, A.; Wiesner, A.; Weinhold, K.; Birmili, W.; Hermann, M.; Merkel, M.; Müller, T.; Pfeifer, S.; Schmidt, A.; Tuch, T.; et al. Mobility particle size spectrometers: Calibration procedures and measurement uncertainties. *Aerosol Sci. Technol.* **2018**, *52*, 146–164. [[CrossRef](#)]
36. Rahman, M.; Mazaheri, M.; Clifford, S.; Morawska, L. Estimate of main local sources to ambient ultrafine particle number concentrations in an urban area. *Atmos. Res.* **2017**, *194*, 178–189. [[CrossRef](#)]
37. Hama, S.M.; Cordell, R.L.; Kos, G.P.; Weijers, E.; Monks, P. Sub-micron particle number size distribution characteristics at two urban locations in Leicester. *Atmos. Res.* **2017**, *194*, 1–16. [[CrossRef](#)]
38. Zhang, T.; Zhu, Z.; Gong, W.; Xiang, H.; Fang, R. Characteristics of Fine Particles in an Urban Atmosphere—Relationships with Meteorological Parameters and Trace Gases. *Int. J. Environ. Res. Public Health* **2016**, *13*, 807. [[CrossRef](#)] [[PubMed](#)]
39. Miao, Y.; Li, J.; Miao, S.; Che, H.; Wang, Y.; Zhang, X.; Liu, S. Interaction between Planetary Boundary Layer and PM_{2.5} Pollution in Megacities in China: A Review. *Curr. Pollut. Rep.* **2019**, *5*, 261–271. [[CrossRef](#)]
40. Buccolieri, R.; Santiago, J.L.; Rivas, E.; Sánchez, B. Reprint of: Review on urban tree modelling in CFD simulations: Aerodynamic, deposition and thermal effects. *Urban For. Urban Green.* **2019**, *37*, 56–64. [[CrossRef](#)]
41. EnelX & Here. City Analytics e Mobility Map. 2020. Available online: <https://enelxmobilityflowanalysis.here.com/dashboard/ITA/info.html> (accessed on 9 April 2020).
42. Conte, M.; Merico, E.; Cesari, D.; Dinoi, A.; Grasso, F.; Donato, A.; Guascito, M.; Contini, D. Long-term characterisation of African dust advection in south-eastern Italy: Influence on fine and coarse particle concentrations, size distributions, and carbon content. *Atmos. Res.* **2020**, *233*, 104690. [[CrossRef](#)]
43. Yaacob, N.F.; Mat, Y.; Muhamad, R.; Abdul, M.; Khairul, N.; Ahmad, B.; Noor, E. A Review of the Measurement Method, Analysis and Implementation Policy of Carbon Dioxide Emission from Transportation. *Sustainability.* 2020, *12*, p. 5873. Available online: <https://www.mdpi.com/2071-1050/12/14/5873> (accessed on 21 July 2020).
44. Dinoi, A.; Weinhold, K.; Wiedensohler, A.; Contini, D. Study of new particle formation events in southern Italy. *Atmos. Environ.* **2021**, *244*, 117920. [[CrossRef](#)]
45. Singh, V.; Singh, S.; Biswal, A.; Kesarkar, A.P.; Mor, S.; Ravindra, K. Diurnal and temporal changes in air pollution during COVID-19 strict lockdown over different regions of India. *Environ. Pollut.* **2020**, *266 Pt 3*, 115368. [[CrossRef](#)]
46. Davidović, M.; Dmitrašinić, S.; Jovanović, M.; Radonić, J.; Jovašević-Stojanović, M. Diurnal, Temporal and Spatial Variations of Main Air Pollutants Before and during Emergency Lockdown in the City of Novi Sad (Serbia). *Appl. Sci.* **2021**, *11*, 1212. [[CrossRef](#)]
47. Brimblecombe, P.; Lai, Y. Diurnal and weekly patterns of primary pollutants in Beijing under COVID-19 restrictions. *Faraday Discuss.* **2020**. [[CrossRef](#)] [[PubMed](#)]
48. Wang, P.; Chen, K.; Zhu, S.; Wang, P.; Zhang, H. Severe air pollution events not avoided by reduced anthropogenic activities during COVID-19 outbreak. *Res. Cons. Rec.* **2020**, *158*, 104814. [[CrossRef](#)] [[PubMed](#)]
49. Huang, X.; Ding, A.; Gao, J.; Zheng, B.; Zhou, D.; Qi, X.; Tang, R.; Wang, J.; Ren, C.; Nie, W.; et al. Enhanced secondary pollution offset reduction of primary emissions during COVID-19 lockdown in China. *Nat. Sci. Rev.* **2020**, *137*. [[CrossRef](#)]